Image-derived indicators of phytoplankton community responses to Pseudo-nitzschia blooms

Vitul Agarwal, Virginie Sonnet, Keisuke Inomura, Audrey Ciochetto, Colleen Mouw

Harmful Algae 138 (2024) 102702

Contents lists available at ScienceDirect

Harmful Algae

journal homepage: www.elsevier.com/locate/hal

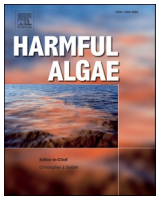

Image-derived indicators of phytoplankton community responses to *Pseudo-nitzschia* blooms

Vitul Agarwal [a,*], Virginie Sonnet [a,b], Keisuke Inomura [a], Audrey B. Ciochetto [a], Colleen B. Mouw [a]

[a] Graduate School of Oceanography, University of Rhode Island, Narragansett, USA
[b] Laboratoire d'Océanographie de Villefanche, Sorbonne Université, CNRS, Villefranche-sur-mer, France

ARTICLE INFO

Edited by Dr. C. Gobler

Original content: Image-derived indicators of phytoplankton community responses to Pseudo-nitzschia blooms (Original data)

Keywords:
Pseudo-nitzschia
Domoic acid
Ecological interactions
Phytoplankton population dynamics
Imaging FlowCytobot (IFCB)
Narragansett Bay

ABSTRACT

Phytoplankton populations in the natural environment interact with each other. Despite rising global concern with *Pseudo-nitzschia* blooms, which can produce the potent neurotoxin domoic acid, we still do not fully understand how other phytoplankton genera respond to the presence of *Pseudo-nitzschia*. Here, we used a 4-year high-resolution imaging dataset for 9 commonly found phytoplankton genera in Narragansett Bay, alongside environmental data, to identify potential interactions between phytoplankton genera and their response to elevated *Pseudo-nitzschia* abundance. Our results indicate that *Pseudo-nitzschia* tends to bloom either concurrently with or right after other phytoplankton genera. Such bloom periods coincide with higher water temperatures and lower salinity. *Pseudo-nitzschia* image abundance tends to increase the most from March-May and peaks during May-Jun, whereas the image-derived biovolume and width of *Pseudo-nitzschia* chains increase the most during Jan-Feb. For most phytoplankton genera, their relationship with *Pseudo-nitzschia* abundance is noticeably different from their relationship with *Pseudo-nitzschia* image features. Despite the complexity in the phytoplankton community, our analysis suggests several ecological indicators that may be used to determine the risk of harmful algal blooms.

1. Introduction

Individual phytoplankton species are influenced by ecological communities and the natural environment. Interactions between different species can take many forms – such as competition for light and nutrient resources (Huisman et al., 1999, 2004; Burson et al. 2018), mixotrophic feeding (Hansen 2011; Stoecker et al. 2017), mutualism by metabolic exchange (Kazamia et al. 2016), growth inhibition due to allelopathy (Legrand et al. 2003) and combined responses to elevated carbon dioxide concentrations (Trimborn et al., 2013; Sampaio et al., 2017). Despite the prevalence of various interactions among co-occurring phytoplankton species, it is often difficult to quantify the strength and effect of ecological interactions from co-occurrence data alone (Cazelles et al., 2016; Freilich et al., 2018; Blanchet et al., 2020). One approach is the creation of a metric, or a family of related indices, that can sufficiently describe the connections between individual taxa (Berlow et al., 1999). Meanwhile, others have proposed using multivariate autoregressive models (Ives et al. 2003) or empirical dynamic models (Deyle et al. 2016) to infer species interactions from reconstructions of system dynamics. The effective characterization of ecological interactions may allow us to develop species-level models for ecological management and enhance the prediction of harmful algal blooms (HABs).

Pseudo-nitzschia can cause HABs under certain conditions, primarily due to the production of the biotoxin domoic acid. Although *Pseudo-nitzschia* is a dominant competitor in various ecosystems, little is known about its relationship with other co-occurring phytoplankton genera. The reasons for its production of domoic acid are also unclear, with competing theories that suggest a role in micronutrient acquisition (Rue and Bruland 2001; Wells et al. 2005; Prince et al. 2013), or as a defense against predation (Lundholm et al., 2018; Olesen et al., 2022). Our understanding of *Pseudo-nitzschia* toxin production is currently limited to laboratory exploration and field sampling. Although culture measurements can allow for the control of confounding variables, they do not sufficiently characterize the inter-specific effects of other phytoplankton taxa on toxin production. Similarly, even though field measurements provide valuable data on extant toxin concentrations, they

* Corresponding author at: Graduate School of Oceanography, University of Rhode Island, Narragansett, USA.
E-mail addresses: vitulagarwal@uri.edu (V. Agarwal), cmouw@uri.edu (C.B. Mouw).

https://doi.org/10.1016/j.hal.2024.102702
Received 21 February 2024; Received in revised form 18 July 2024; Accepted 24 July 2024
Available online 31 July 2024

rely exclusively on the availability of funding and can often fail to capture the short-term dynamics of *Pseudo-nitzschia* populations.

One approach to circumvent these limitations is by developing descriptive relationships between domoic acid production and potential environmental triggers. To this end, one recent study has attempted to describe the environmental covariates of domoic acid production (Sterling et al., 2022). Unfortunately, as domoic acid production can be strain-specific and intermittent (Bates et al. 2018; Dong et al. 2020; Sandoval-Belmar et al. 2023), changes in the abundance of *Pseudo-nitzschia*, at the genus level, do not act as a reliable predictor of domoic acid production. A possible solution to this problem is the development of indicators that leverage other ecological data present within the same environment – such as the abundance of other phytoplankton genera.

In this study, we use a high-resolution, daily-scale dataset of Imaging FlowCytobot (IFCB) images deployed in Narragansett Bay from Jun-2017 to Oct-2021. We first generate a multivariate time series of the proxy planktonic abundance for nine phytoplankton genera. We then utilize a simple mathematical approach to quantify the "interactions" between *Pseudo-nitzschia* and eight other planktonic groups, which relate to the timing of blooms and any relative changes in abundance. We answer the following questions: [1] How does the phytoplankton community change in response to *Pseudo-nitzschia* blooms? and [2] Are there image indicators of harmful algal bloom risk in *Pseudo-nitzschia*?

2. Materials and methods

2.1. Imaging flowcytobot

All the phytoplankton time series used in this study were collected by deploying an Imaging FlowCytobot (IFCB) in Narragansett Bay, Rhode Island, at the end of a pier (41.492°N, 71.419°W). We used daily aggregated IFCB data from 14th June 2017 to 20th October 2021. Image concentration $\left(\#\ images\ mL^{-1}\right)$ was calculated by dividing the average daily number of images by the average sampling volume. All missing data points were approximated using 30-day exponential moving averages (EMA) computed by the R package "imputeTS" (Moritz and Bartz-Beielstein, 2017). Discussion on the limits of the IFCB, data preprocessing, and the use of image concentration as a proxy for abundance, can be found in prior studies on the morphology and predictability of phytoplankton populations in Narragansett Bay (Sonnet et al., 2022; Agarwal et al., 2023).

We selected nine phytoplankton genera from the IFCB dataset that are commonly found in Narragansett Bay and could be identified via a random forest classifier (Sosik and Olson 2007) that was developed in-house from a library of manually annotated images from our dataset (refer to Sonnet et. al. 2022 for classifier development and application). Table 1 reports the sensitivity and precision scores of the random forest classifier for each of the nine phytoplankton genera that were included. For classes included in the classifier, both scores were calculated on all images that were manually classified. This excludes the training set of images used to create the classifier and all images that were unclassified (i.e. the probability of an image belonging to any specific class was too low). Fig. 1 illustrates some IFCB images for the phytoplankton genera.

Table 1
Sensitivity and precision of the automatic classifier for each of the phytoplankton classes

	Sensitivity	Precision
Pseudo-nitzschia (N=344)	0.86	0.91
Dinophysis (N=177)	0.95	0.91
Chaetoceros (N=2260)	0.80	0.95
Skeletonema (N=1257)	0.91	0.87
Ditylum (N=1163)	0.98	0.98
Eucampia (N=2450)	0.93	0.98
Leptocylindrus (N=362)	0.91	0.63
Rhizosolenia (N=522)	0.87	0.77
Pyramimonas (N=210)	1.00	0.73

$$Sensitivity = \frac{TP}{TP + FN} \tag{1}$$

$$Precision = \frac{TP}{TP + FP} \tag{2}$$

where TP, FP and FN are the number of true positive, false positive, and false negative images respectively.

To evaluate seasonal changes in phytoplankton population abundance, we created a time series of daily change for each of the nine phytoplankton genera. First, each time series was standardized (z-scored) by subtracting the mean and dividing by the standard deviation of the time series. Second, change was calculated for each day between 14th June 2017 to 20th October 2021 by subtracting the abundance of the genus on the previous day ($\Delta x_t = x_t - x_{t-1}$). Lastly, the time series of daily change was averaged to monthly time scales to provide an estimate of mean monthly change in abundance across the entire time period. The mean monthly change in abundance was visualized using two different techniques. First, we plotted the change in each month as a bar plot to highlight the relative differences in the magnitude of change. Second, we used the same data to create dynamical barcodes (Agarwal and Mouw, 2022). In brief, this method assigns a color scheme to the direction, not the magnitude, of change from month to month. Similarities in the barcode indicate that the phytoplankton genera were in sync with each other over the length of the time series, regardless of the magnitude of the relative changes.

2.2. Image features

236 image features can be derived from every IFCB image (Sosik and Olson, 2007, https://github.com/hsosik/ifcb-analysis/wiki). We created a time series for a limited set of image features for *Pseudo-nitzschia*, based on their potential relevance to phytoplankton ecology, as described in Agarwal et. al. 2023 with no modifications. The time series were created by calculating the average daily values for the image features and scaled by the average sampling volume for each day. As *Pseudo-nitzschia* is a chain-forming species, image concentration may not reveal the true abundance of the genus in the environment. To support our investigation into the relationships between phytoplankton genera, we used the image features 'minor axis' and 'biovolume' to provide additional context on *Pseudo-nitzschia* presence at the sampling location. 'Minor axis' approximates the cell width of observed *Pseudo-nitzschia* chains whereas 'biovolume' approximates their overall size. For each analysis conducted with the time series of *Pseudo-nitzschia* abundance, we repeated the analysis with the time series of *Pseudo-nitzschia* 'biovolume' and 'minor axis'.

2.3. Environmental data

Daily averages of water temperature $(^{\circ}C)$, chlorophyll concentration $(\mu g\ L^{-1})$, salinity (ppt), and pH were requested from the Narragansett Bay Fixed Site Monitoring Network (NBFSMN, personal communication: Heather Stoffel). These measurements were co-located with the Imaging FlowCytobot. Daily averages of wind speed $(m\ s^{-1})$ and tidal height (Mean Sea Level; m) were calculated from measurements at the NOAA Quonset Point Buoy (41° 35.2 N, 71° 24.6 W; #8454049; https://tidesandcurrents.noaa.gov/).

The environmental data were analyzed in relation to changes in *Pseudo-nitzschia* proxy abundance. Each environmental time series was divided into 'bloom' periods and 'non-bloom' periods. Daily changes that exceeded three times the median of the *Pseudo-nitzschia* time series were considered 'bloom periods'. We then compared the mean, standard deviation, and standard error of the environmental parameters for both these periods. For the second part of the analysis, we used an interaction

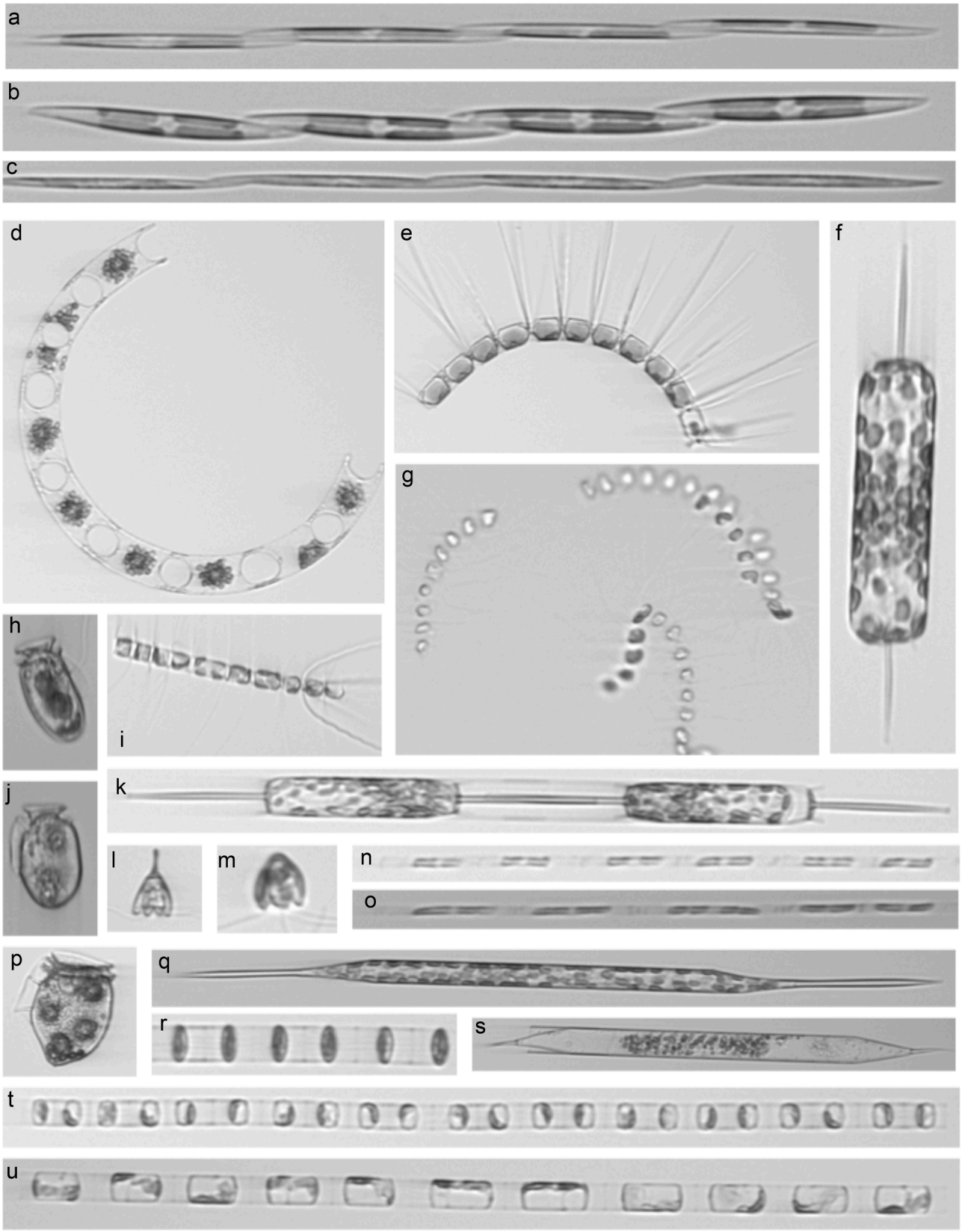

Fig. 1. Illustrative images taken by the imaging flowcytobot deployed in Narragansett Bay, Rhode Island (41.492°N, 71.419°W). [a,b,c] *Pseudo-nitzschia*, [d] *Eucampia*, [e,g,i] *Chaetoceros*, [f,k] *Ditylum*, [h,j,p] *Dinophysis*, [l,m] *Pyramimonas*, [n,o] *Leptocylindrus*, [q,s] *Rhizosolenia*, [r,t,u] *Skeletonema*.

metric (described below) to check for relevant differences between the abundance of *Pseudo-nitzschia* and its image features. Lastly, the time series of temperature was also used to understand the seasonal patterns of *Pseudo-nitzschia* abundance and image features, where the dataset was divided into three periods – below 8°C, 8–16°C and greater than 16°C.

2.4. Interaction metric

To help understand differences in bloom phenology, we defined an interaction metric based on the average abundance of one species when another species increases or decreases in abundance:

$$\text{Interaction Strength } (\mathbf{x}\rightarrow\mathbf{y}) = \frac{\text{mean of species } \mathbf{x} \text{ (for points where abundance for species } \mathbf{y} \text{ went up in the next time step)}}{\text{mean of species } \mathbf{x} \text{ (for points where abundance for species } \mathbf{y} \text{ went down in the next time step)}} - 1$$

For this metric, one is subtracted to center the metric around zero. Negative interactions indicate that the mean abundance of species **x** was greater when species **y** was decreasing in abundance. Conversely, positive interactions indicate that the mean abundance of species **x** was greater when species **y** was increasing in abundance. Although this metric is focused on identifying trends in population growth patterns and does not imply causality, it may be used to infer relationships between species **x** and **y**. For example, a negative interaction may occur when species **x** *causes*, either directly or indirectly, the decrease in abundance in species **y**. Greater the value of the metric (whether positive or negative), greater is the potential interaction between species **x** and species **y**.

We tested this metric on simulated blooms of two phytoplankton species, defined as Gaussian distributions of abundance with varying magnitude and standard deviation (bloom duration). We also simulated some error within the distributions by adding random noise to 10 % of the distribution. Values for noise were selected from a uniform distribution (min $= 0$, max $= 20$). Figure S1 highlights some examples of the interaction metric for the 2 model species. The interaction metric is typically 0 in both directions (x→y **and** y→x) when there is either complete overlap or no overlap between 2 species regardless of relative magnitude and duration. In all other cases, the metric can take different values depending on relative magnitude and any differences in bloom duration. As real time series likely have multiple peaks over many years with varying bloom durations, the interaction metric provides only an average estimate of how abundant one species typically is when another species is increasing or decreasing in abundance. Even though the metric can theoretically take any value, real time series typically show relationships between -1 and 1.

2.5. Software

All the analyses were conducted in R Core Team (2021). For plotting and data visualization, we used the R packages "ggplot2" (Wickham 2016) and "cowplot" (Wilke, 2020). Features of IFCB images were analyzed and extracted using the MATLAB-based IFCB Analysis custom toolbox (Sosik, https://github.com/hsosik/ifcb-analysis). IFCB images were classified with a random-forest algorithm developed and applied in MATLAB utilizing the Statistic and Machine Learning Toolbox.

3. Results

The time series of each phytoplankton genus showed intermittent periods of rapid increase and decrease in image concentration from Jun-2017 to Oct-2021 (Fig. 2). There were marked differences in the scale of proxy abundance. Some taxa (e.g. *Chaetoceros* or *Skeletonema*) were an order of magnitude higher than other taxa (e.g. *Dinophysis* or *Ditylum*). On average, there were no negative correlations between the time series,

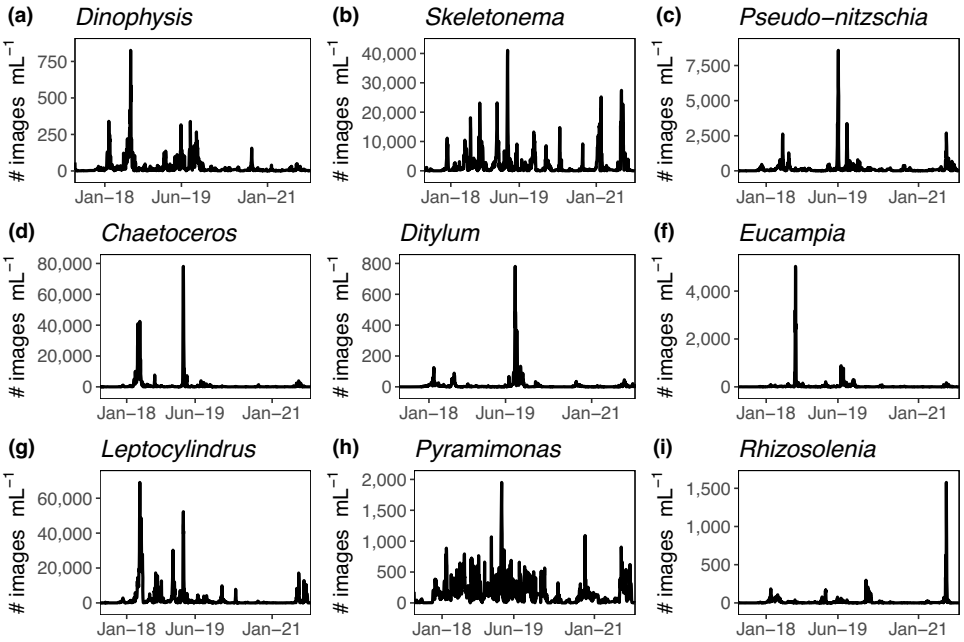

Fig. 2. Time series of nine phytoplankton genera in Narragansett Bay, Rhode Island. Abundance is estimated from the number of unique images taken by the IFCB and classified as (a) *Dinophysis*, (b) *Skeletonema*, (c) *Pseudo-nitzschia*, (d) *Chaetoceros*, (e) *Ditylum*, (f) *Eucampia*, (g) *Leptocylindrus*, (h) *Pyramimonas*, and (i) *Rhizosolenia*. Note: As some of these genera are chain-forming, image concentration is only a proxy for their true abundance.

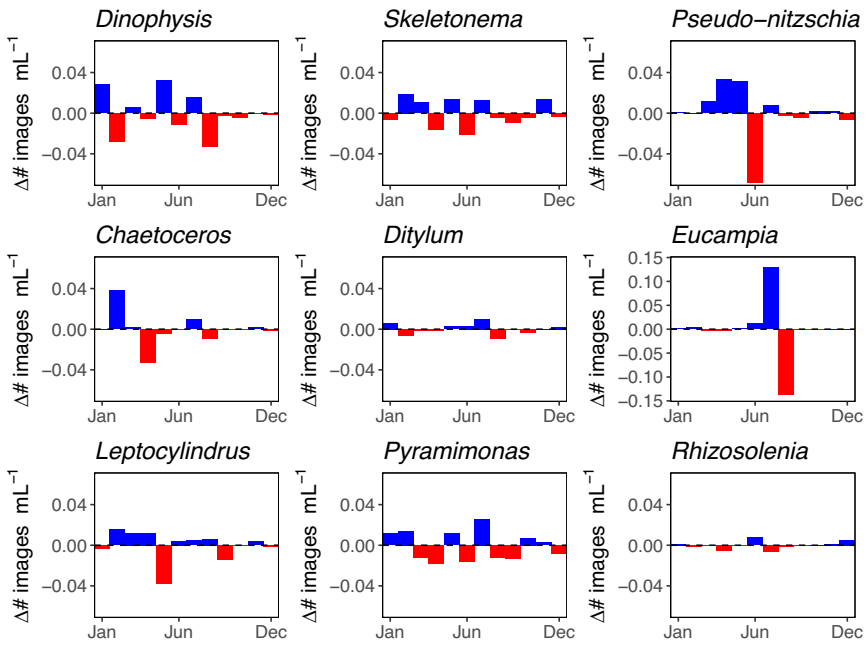

Fig. 3. Mean monthly change in standardized image concentration $(\Delta\#\ images\ mL^{-1})$ for nine phytoplankton genera in Narragansett Bay, Rhode Island. Each time series was standardized (z-scored) by subtracting the mean and dividing by the standard deviation of the time series. Blue indicates positive values and red indicates negative values. Each bar represents a monthly average of daily changes starting from January (left) to December (right). Note: The y-axis scale for *Eucampia* is different from the others. As some of these genera are chain-forming, image concentration is only a proxy for their true abundance.

with most genera exhibiting weak-but-positive correlation coefficients (Fig. S2).

When we aggregated daily-scale changes to seasonal cycles (Fig. 3), it was apparent that the success of many phytoplankton genera was tied to specific months of the year. For example, *Pseudo-nitzschia* has its greatest increase during Spring (March-May) and rapidly decreases in relative abundance during June (Fig. 3c). Similarly, *Eucampia* is a strong summer-blooming species as relative change is highest for the month of July, which is immediately followed by a strong drop in abundance during August (Fig. 3f). Other genera, such as *Dinophysis, Skeletonema*,

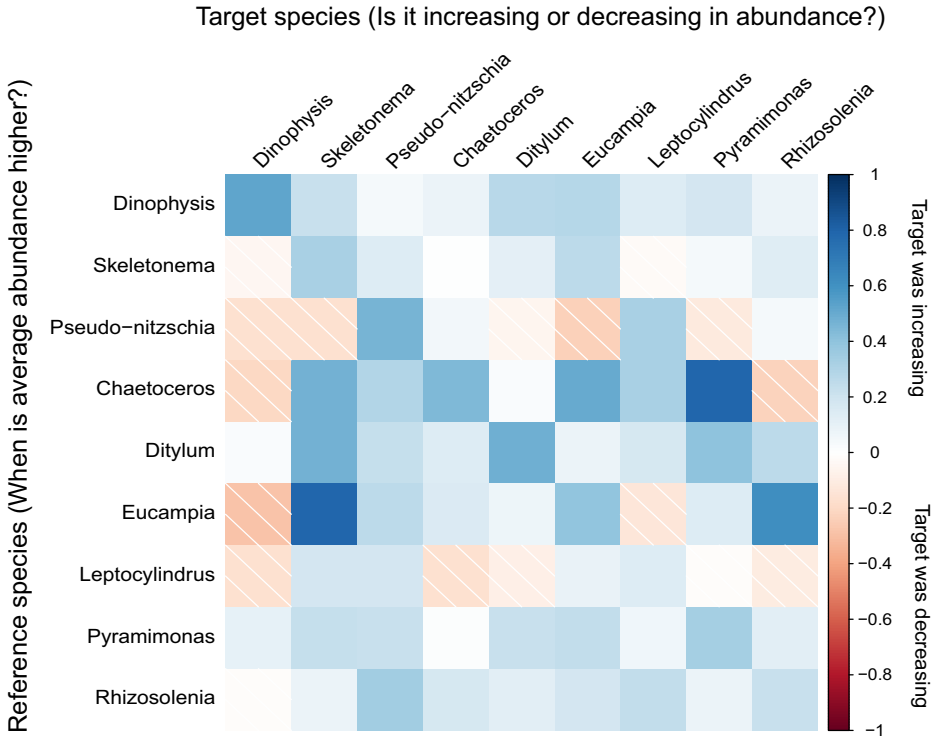

Fig. 4. Estimating the relationships between different phytoplankton genera in Narragansett Bay using an interaction metric (see *Methods*). Rows indicate the reference species and columns indicate the target species. Negative values (red and hatching) show that the reference species typically bloomed after the target. Note: The diagonal of the matrix is positively biased due to the asymmetric nature of most phytoplankton blooms (slow increases followed by rapid decreases). Note: As some of these genera are chain-forming, image concentration is only a proxy for their true abundance.

and *Pyramimonas*, show switching between periods of increase and decrease every 1–2 months (Fig. 3a, b, h). *Ditylum* and *Rhizosolenia* seemed to be relatively consistent in daily change across the year, with lower increases and decreases when compared to other genera (Fig. 3e, i). When evaluated for directional similarities in seasonal change (i.e. focusing on direction rather than magnitude of change), dynamical barcodes revealed extensive similarities between phytoplankton genera, such as *Pseudo-nitzschia* and *Pyramimonas* during the months of June to December (Figure S3; Agarwal and Mouw, 2022).

We developed an interaction metric that broadly described the relationships in phytoplankton bloom phenology, daily changes in phytoplankton abundance, and the relative rates of increase and decrease across different taxa. For our nine genera in Narragansett Bay, the metric ranged from -1 – 1 (Fig. 4). *Pseudo-nitzschia* had a unique signature when compared to other genera, with a greater number of negative interactions (Fig. 4; row 3). The mean of *Pseudo-nitzschia* was higher when *Dinophysis, Skeletonema, Ditylum, Eucampia*, and *Pyramimonas*, were decreasing in abundance rather than when these genera were increasing in abundance. In contrast, most phytoplankton genera had a positive interaction metric in response to *Pseudo-nitzschia* (Fig. 4; column 3), suggesting that their mean abundance was higher when *Pseudo-nitzschia* was increasing in abundance rather than when *Pseudo-nitzschia* was decreasing in abundance. Interestingly, all the phytoplankton genera had blooms that were asymmetric. The positive values on the diagonal in Fig. 4 suggest that periods where abundance is increasing have higher mean values than the periods where abundance is decreasing.

Our analysis of relevant environmental parameters revealed that external conditions were mostly consistent during *Pseudo-nitzschia* bloom and non-bloom periods (Fig. 5). A notable exception was water temperature, which tends to be higher than average ($p < 0.01$ on a Welch Two-Sample t-test) and lower in variability during periods of *Pseudo-nitzschia* blooms. Salinity is slightly lower than average ($p < 0.01$ on a Welch Two-Sample t-test) during *Pseudo-nitzschia* blooms.

When we looked at the seasonality of features as derived from the IFCB images (Fig. 6), we found that *Pseudo-nitzschia* species tend to be thinner than average during periods of rapid increase in Mar-May (Fig. 6c), and thicker than average during February and June. Both the width (minor axis) and biovolume are greatest when temperatures are 16–25°C, whereas total abundance is typically higher when temperatures are 8–16°C (Fig. 7, $p < 0.01$ on a Welch Two-Sample t-test).

Image features, such as the width and biovolume, also varied differently in relation to other phytoplankton genera as compared to *Pseudo-nitzschia* abundance (Fig. 8). Even though *Pseudo-nitzschia* abundance is greater when *Skeletonema, Ditylum, Eucampia* and *Pyramimonas* are decreasing in abundance (Fig. 4), both *Pseudo-nitzschia* width and biovolume are marginally greater when those genera are increasing in abundance. *Pseudo-nitzschia* abundance is also much higher when *Leptocylindrus* abundance is increasing, but the relationship between the image features and *Leptocylindrus* is much weaker (i.e. the interaction metric is much lower). In contrast, the results for *Dinophysis* point to the opposite trend. *Pseudo-nitzschia* abundance is higher when *Dinophysis* is decreasing in abundance, but the relationship is weaker between the image features and abundance of *Dinophysis*. The estimated differences with environmental variables were relatively weak across all cases.

4. Discussion

4.1. How do other phytoplankton genera respond to Pseudo-nitzschia blooms?

Phytoplankton populations in the natural environment are subject to environmental and ecological influence. Although previous studies in Narragansett Bay have studied individual genera in detail, such as *Thalassiosira* (Rynearson et al. 2020) and *Pseudo-nitzschia* (Roche et al. 2022), little has been known about changes in community composition at a daily-scale resolution. The time series of each phytoplankton genus exemplifies a highly dynamic environment where there may often be interactions between different genera. The difference in abundance scale between the nine phytoplankton genera, particularly at the peak of a bloom, suggests that some genera are more competitive during rapid growth periods and can achieve greater genus-level biomass under favorable conditions.

When we attempted to understand the relationship between different genera based on an interaction metric, we found that *Pseudo-nitzschia* is somewhat unique. On average, greater abundance of *Pseudo-nitzschia* was coincident with a decrease in abundance in many other taxa. In

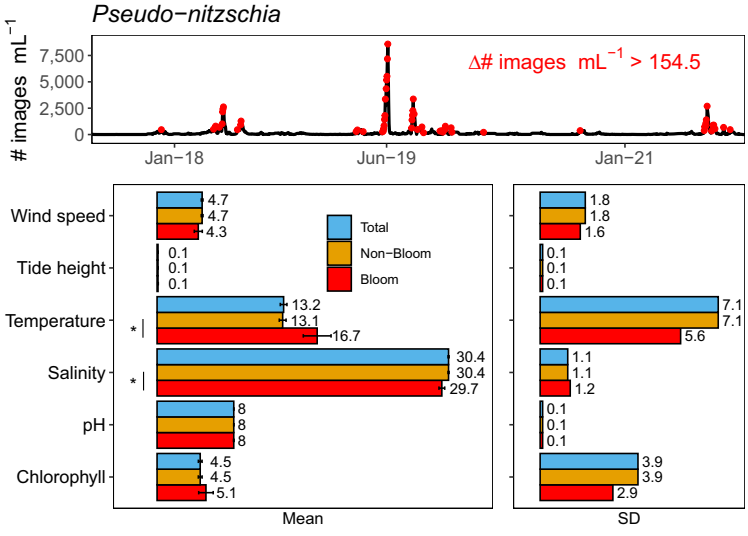

Fig. 5. Environmental factors and how they relate to *Pseudo-nitzschia* bloom periods. The top panel shows the time series of *Pseudo-nitzschia* image concentration with the red points indicating the events where the daily change exceeded 154.5 images mL^{-1} (defined as "bloom periods"; 3 times the median of the time series). The bottom panels show the mean (left) and standard deviation (right) of wind speed ($m\ s^{-1}$), tide height (m), water temperature ($^{\circ}C$), salinity (ppt), pH and chlorophyll ($\mu g\ L^{-1}$) in Narragansett Bay that coincided with the bloom periods (red), non-bloom periods (gold) and the entire time series (blue). Error bars around the mean represent 95 % confidence intervals ($1.96 \times S.E.$). * indicates $p < 0.01$ on a Welch Two-Sample t-test.

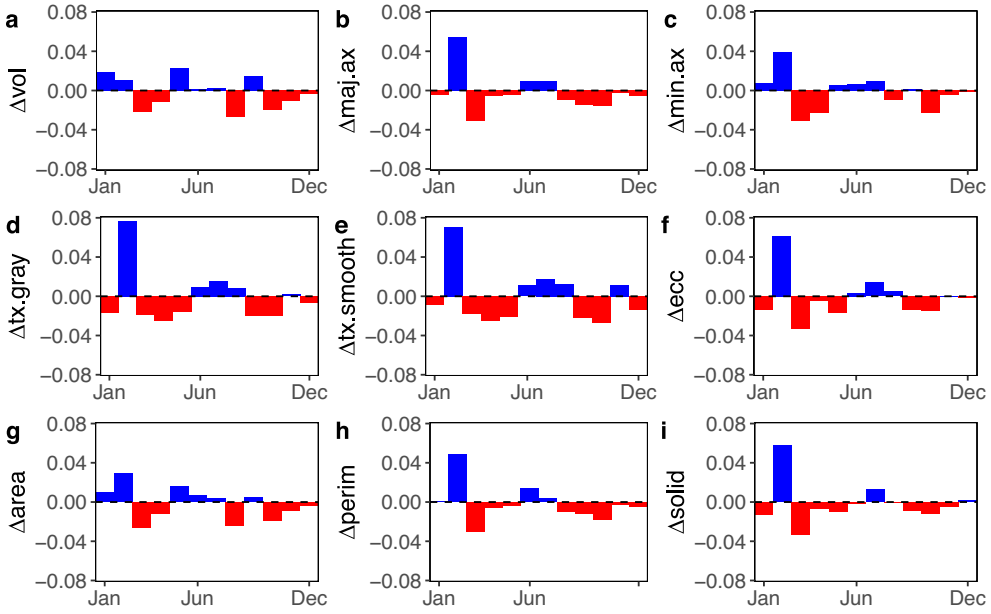

Fig. 6. Mean monthly change in standardized features for *Pseudo-nitzschia* in Narragansett Bay, Rhode Island. Each time series was standardized (z-scored) by subtracting the mean and dividing by the standard deviation of the time series. Blue indicates positive values and red indicates negative values. Each bar represents a monthly average of daily changes starting from January (left) to December (right). vol – biovolume, maj.ax – major axis length, min.ax – minor axis length, tx.gray – texture gray, tx.smooth – texture smooth, ecc – eccentricity, area – surface area, perim – perimeter, solid – solidity (Sosik and Olson 2007, https://github.com/hsosik/ifcb-analysis/wiki).

contrast, other genera were greater in abundance when *Pseudo-nitzschia* was increasing rather than when it was decreasing. The direction of this interaction likely points towards a succession-based bloom structure where *Pseudo-nitzschia* abundance maxima follow those of other genera. Other studies conducted in different regions have found a similar structure in *Pseudo-nitzschia* blooms, i.e. the genus tends to appear concurrently or immediately after the decrease of other phytoplankton species (Delegrange et al., 2018; Houliez et al., 2023).

Given that most phytoplankton blooms were also asymmetric (i.e. there are longer periods of increasing abundance and shorter periods of decreasing abundance), our results signal the existence of a physiological, ecological, or environmental mechanism that allows *Pseudo-nitzschia* to outperform its competitors. One possibility could be changing environmental conditions, which likely confer a competitive advantage to *Pseudo-nitzschia* during certain time periods of the year. Although we noticed only minor differences in environmental variables during *Pseudo-nitzschia* blooms and non-blooms, it is probable that the effects of the environment are strongest on the niches of different species and less so on the niche of the genus, as seen in the differences among image features. Studies on other phytoplankton genera suggest that niche optimums for temperature can differ greatly among and within different species, strains and ecotypes within the same genus (Anderson and Rynearson, 2020; Smith et al., 2021; Bishop et al., 2022; Roche et al., 2022). Another possibility could be the presence of a mechanism that either promotes growth in *Pseudo-nitzschia* or subdues the growth of other genera. This could occur directly through some form of cell-to-cell signaling with infochemicals between phytoplankton and other microbes (Amin et al. 2015; Koester et al. 2022) or the allelopathic inhibition of competitor growth (Xu et al., 2015). Alternatively, indirect mechanisms of interaction between *Pseudo-nitzschia* and other genera include changing predator behavior (Lundholm et al. 2018; Olesen et al. 2022) and effective competition under iron or copper limitations (Rue and Bruland, 2001; Wells et al., 2005; Prince et al., 2013).

4.2. Are there image indicators of harmful algal bloom risk in Pseudo-nitzschia?

Domoic acid is a potent biotoxin that is produced by some *Pseudo-nitzschia* species, including those found in Narragansett Bay (Sterling et al., 2022). Part of the global concern with *Pseudo-nitzschia* blooms are the general effects of domoic acid on birds and mammals (Fritz et al. 1992; Fire et al. 2011), and its potential to cause amnesic shellfish poisoning in humans (Bates et al. 1989). Consequently, multiple recent studies across the world have focused on mapping the distribution of toxin-producing species (Dong et al. 2020; Cembella et al. 2023), studying the environmental factors that might be associated with domoic acid production (Likumahua et al., 2019; Kelly et al. 2023; Sandoval-Belmar et al. 2023), understanding relevant physiological mechanisms (Sauvey et al. 2023; Xu et al. 2023), and the potential role of marine pollutants (Bretherton et al., 2019). The natural responses of phytoplankton communities to domoic acid production; however, are less explored, even though experimental evidence suggests that there exist both direct and indirect effects on other phytoplankton (Prince et al., 2013; Xu et al., 2015). The identification of repeatable specific community responses could be an asset for ecological monitoring in areas where *Pseudo-nitzschia* is known to exist, but frequent domoic acid measurements are neither feasible nor economical. For such areas, the risk of harmful algal blooms could be modulated by consistently monitoring changes in the phytoplankton communities themselves for any tell-tale signs of domoic acid presence.

Despite the lack of domoic acid data, we attempted to indirectly infer the risk of domoic acid presence by studying the relationship between the image features of *Pseudo-nitzschia* and other phytoplankton genera. As different *Pseudo-nitzschia* species have different morphological characteristics (Stonik et al. 2001; Ljubešić et al. 2011; Louw et al. 2018), the use of image features such as width and biovolume can offer some insight into the species-level dynamics in the absence of species-specific information. IFCB images do not provide enough detail to discriminate between different *Pseudo-nitzschia* species, but previous studies have associated variability in image features to dynamic shifts on a species level (Hubbard et al., 2023). Domoic acid concentrations in

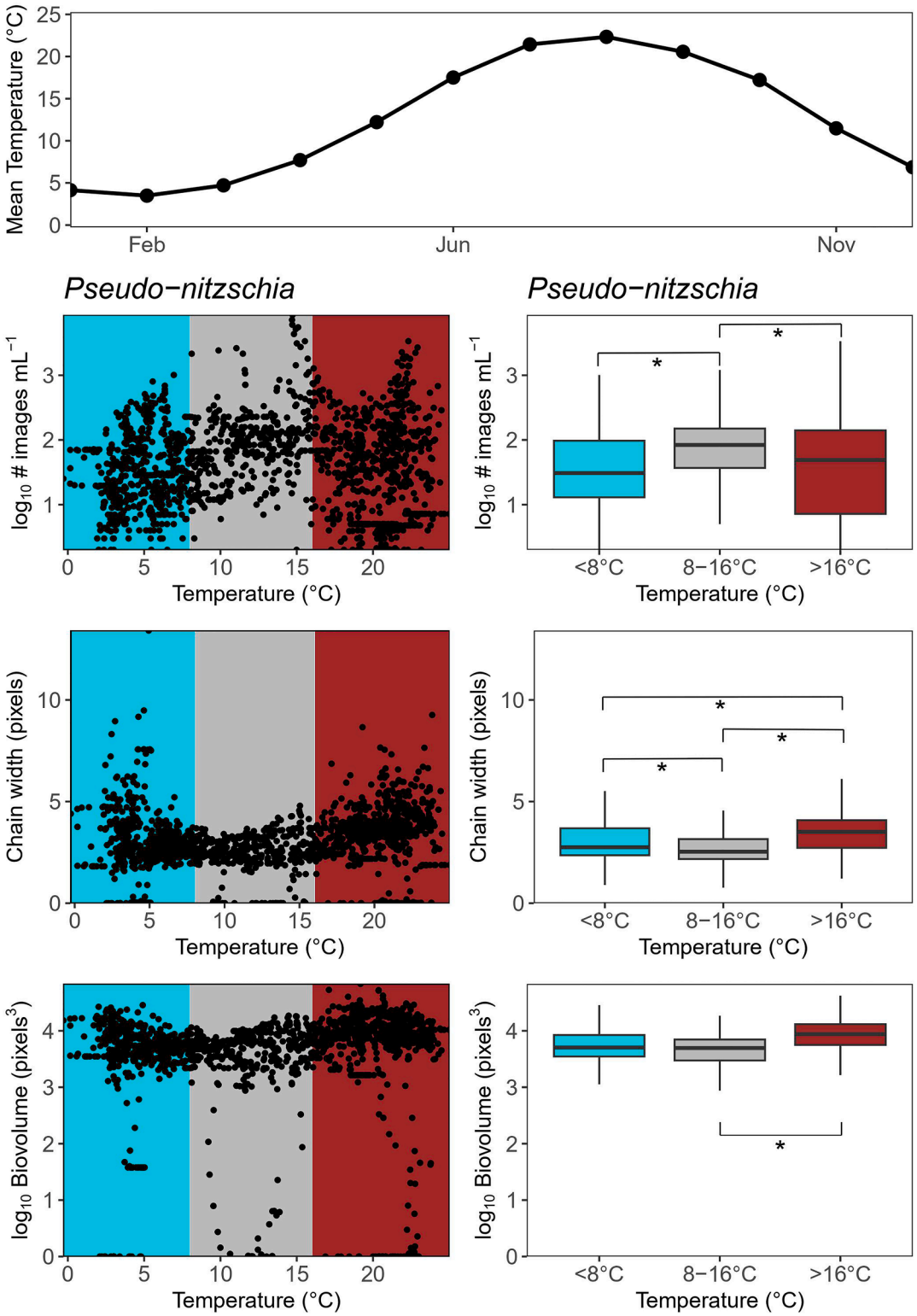

Fig. 7. Relationship between water temperature (°C) and *Pseudo-nitzschia* abundance (top left), chain width (minor axis length; middle left) and biovolume (bottom left). The panels on the right are the same data but visualized as boxplots. The top panel indicates the average monthly temperature from June-2017 – October-2021. Cyan shading refers to periods where the temperature was under 8°C. Red shading refers to periods where the temperature was greater than 16°C. * indicates $p <$ 0.01 on a Welch Two-Sample t-test.

Narragansett Bay are typically greatest in the Summer and Fall seasons (Sterling et al., 2022). Interestingly, both the width and biovolume of *Pseudo-nitzschia* chains show similar patterns over this time period. The months of May-July were marked by increases in biovolume and width, followed by a decrease in August and a subsequent increase in September. Coincidentally, August is the month in Narragansett Bay when temperatures are the highest. Many of these differences are likely driven by some species-specific properties of *Pseudo-nitzschia* and highlight the potential role of some toxigenic species (Roche et al., 2022). For example, the sharpest increase in width was during the

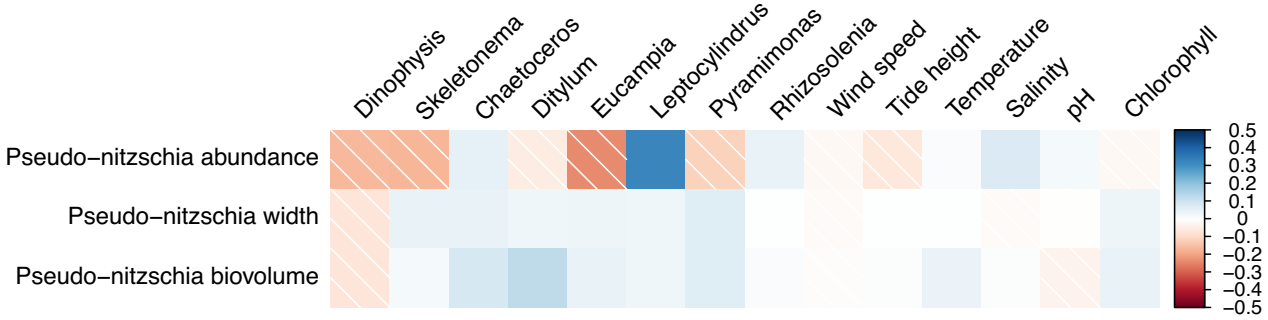

Fig. 8. The estimated width and biovolume of *Pseudo-nitzschia* chains vary differently from its abundance. The values are calculated from the interaction metric (see *Methods*). Positive values (blue) indicate that the abundance, width or biovolume of *Pseudo-nitzschia* was greater when the abundance of the target species (or the associated environmental factor) was increasing. Negative values (red and hatching) indicate that the abundance, width or biovolume of *Pseudo-nitzschia* was greater when the abundance of the target species (or the associated environmental factor) was decreasing.

month of February, which is coincident with the presence of *Pseudo-nitzschia australis* (Roche et al. 2022), a domoic acid producing species that can be 'wider' than others (Sterling et al., 2022). It should be noted, however, that there can be several exceptions to the association between width and domoic acid risk. Determining true risk will likely require instrumentation that can combine high-resolution imaging with automated species or strain-level identification.

The proxy abundance of *Pseudo-nitzschia* was much higher when *Leptocylindrus* was increasing, but the width and biovolume of *Pseudo-nitzschia* were relatively the same. For most other genera we tested, the difference in results between the image features and proxy abundance was in the positive direction, i.e., the width and biovolume of *Pseudo-nitzschia* were higher when the abundance of other genera was increasing. These inverse relationships reveal a general pattern – *Pseudo-nitzschia* species with lower width and biovolume account for a larger proportion of total *Pseudo-nitzschia* abundance. Large increases or decreases in proxy abundance mostly reflects the behavior of the 'thinner' species. This also suggests that the 'thicker' *Pseudo-nitzschia* species may have differential effects on other phytoplankton genera. In the case of *Leptocylindrus*, the 'thinner' species is associated with increasing *Leptocylindrus* abundance whereas the 'thicker' species is not. In contrast, the 'thinner' species of *Pseudo-nitzschia* is associated with decreasing *Dinophysis* abundance (or, is succeeding *Dinophysis* blooms), but the 'thicker' species has less of an effect. Future studies may need to carefully evaluate the physiological or ecological mechanisms for this relationship, as *Dinophysis* and *Pseudo-nitzschia* co-exist in a number of global marine ecosystems (Velo-Suárez et al., 2008; Seeyave et al., 2009; Ajani et al., 2013; Wohlrab et al., 2020; Lima et al., 2022; Díaz et al., 2023).

4.3. Study limitations and future directions

There are several methodological choices within this study that merit further consideration. First, even though we utilize an interaction metric, our implementation was largely aimed at describing a very large imaging dataset for nine phytoplankton genera. Each value was derived from four years of a daily-scale time series and does not necessarily imply a mechanistic explanation between any two phytoplankton genera. As such, interaction coefficients are only meant to provide summarized information on any general trends. Second, each time series likely contains some sources of error (measurement, identification, processing etc.). Monitoring programs may need to systematically evaluate such sources of error for the development of harmful algal bloom indicators. Third, our focus in this paper was on identifying trends and reporting cohesive observations. Future studies may need to continue long-term observations and conduct culture experiments to conclusively report on the effects of *Pseudo-nitzschia* (and in some cases, domoic acid) on other phytoplankton genera.

5. Conclusions

Harmful algal blooms (HABs) are an increasing threat to human health, fisheries, and tourism. To successfully predict HABs caused by *Pseudo-nitzschia*, a cosmopolitan diatom that can produce domoic acid, current strategies require extensive field sampling and monitoring for toxin production. In this study, we tested an alternative approach to traditional phytoplankton manual counts and utilized a full community analysis to indicate risk of *Pseudo-nitzschia* blooms. Using a 4-year daily resolution dataset collected with an Imaging FlowCytobot (IFCB), we created a mathematical metric to evaluate the relative changes in abundance for 9 phytoplankton genera in relation to changes in *Pseudo-nitzschia* abundance, width and biovolume. We also evaluated differences in environmental variables to understand the context of *Pseudo-nitzschia* blooms.

Patterns in *Pseudo-nitzschia* abundance indicated that the genus typically blooms concurrently with or right after other phytoplankton genera. Interestingly, *Pseudo-nitzschia* width and biovolume, both variables that can be associated with species-level change and domoic acid risk, show different patterns when compared to abundance. This suggests that *Pseudo-nitzschia* abundance may be relevant for harmful algal bloom prediction, but the monitoring of other metrics such as width and biovolume may indicate periods where domoic acid risk is greater than average. There is significant species diversity within the genus *Pseudo-nitzschia* and some water temperatures may be more likely to host species-of-concern. The warmest water temperatures (16-25°C) were when high *Pseudo-nitzschia* abundance, high chain width and high estimated biovolume were observed. Other ecological indicators for monitoring harmful algal bloom risk could be the abundance of genera such as *Dinophysis, Leptocylindrus* and *Pyramimonas*, which show some evidence of common drivers with *Pseudo-nitzschia* and the possibility of inter-species interactions. For the development of early-warning systems that are high-resolution, autonomous, and rely on singular data sources, our analysis suggests the inclusion of ecological and environmental indicators that may serve to enhance information quality for prediction models.

CRediT authorship contribution statement

Vitul Agarwal: Writing – review & editing, Writing – original draft, Visualization, Validation, Software, Methodology, Investigation, Formal analysis, Data curation, Conceptualization. **Virginie Sonnet:** Writing – review & editing, Visualization, Validation, Methodology, Data curation. **Keisuke Inomura:** Writing – review & editing, Validation, Supervision, Methodology, Investigation, Funding acquisition, Conceptualization. **Audrey B. Ciochetto:** Writing – review & editing, Resources, Project administration, Methodology, Data curation. **Colleen B. Mouw:** Writing – review & editing, Supervision, Resources, Project

administration, Funding acquisition, Conceptualization.

Declaration of competing interest

The authors declare that they have no known competing financial interests or personal relationships that could have appeared to influence the work reported in this paper.

Data availability

Image-derived indicators of phytoplankton community responses to Pseudo-nitzschia blooms (Original data) (Zenodo).

Acknowledgements

VA and CBM acknowledge support from the Rhode Island Sea Grant (Grant number: NA22OAR4170123 to CBM). CBM acknowledges support from CINAR (Cooperative Institute for the North Atlantic Region; Grant number: NA19OAR4320074 to CBM). VS acknowledges support from NASA FINESST (80NSSC20K1638 awarded to VS and CBM). This work was supported by a grant from the Simons Foundation (LS-ECIA-MEE-00001549 to KI). We thank Heather Stoffel for the provision of environmental data, and Matthew J. Bertin and Katherine M. Roche for their comments on earlier versions of this paper.

Supplementary materials

Supplementary material associated with this article can be found, in the online version, at doi:10.1016/j.hal.2024.102702.

References

Agarwal, V., Chávez-Casillas, J., Mouw, C.B., 2023. Sub-monthly prediction of harmful algal blooms based on automated cell imaging. Harmful Algae 122, 102386. https://doi.org/10.1016/j.hal.2023.102386.

Agarwal, V., Mouw, C.B., 2022. Barcoding and its application for visualizing ecological dynamics. bioRxiv. https://doi.org/10.1101/2022.04.07.487508.

Ajani, P., Brett, S., Krogh, M., Scanes, P., Webster, G., Armand, L., 2013. The risk of harmful algal blooms (HABs) in the oyster-growing estuaries of New South Wales. Australia. Environ. Monit. Assess. 185, 5295–5316. https://doi.org/10.1007/s10661-012-2946-9.

Amin, S.A., Hmelo, L.R., Van Tol, H.M., Durham, B.P., Carlson, L.T., Heal, K.R., Morales, R.L., Berthiaume, C.T., Parker, M.S., Djunaedi, B., Ingalls, A.E., Parsek, M. R., Moran, M.A., Armbrust, E.V., 2015. Interaction and signalling between a cosmopolitan phytoplankton and associated bacteria. Nature 522, 98–101. https://doi.org/10.1038/nature14488.

Anderson, S.I., Rynearson, T.A., 2020. Variability approaching the thermal limits can drive diatom community dynamics. Limnol. Oceanogr. 65, 1961–1973. https://doi.org/10.1002/lno.11430.

Bates, S.S., Bird, C.J., de Freitas, A.S.W., Foxall, R., Gilgan, M., Hanic, L.A., Johnson, G. R., McCulloch, A.W., Odense, P., Pocklington, R., Quilliam, M.A., Sim, P.G., Smith, J. C., Subba Rao, D.V., Todd, E.C.D., Walter, J.A., Wright, J.L.C., 1989. Pennate diatom *Nitzschia pungens* as the primary source of domoic acid, a toxin in shellfish from Eastern Prince Edward Island, Canada. Can. J. Fish. Aquat. Sci. 46, 1203–1215. https://doi.org/10.1139/f89-156.

Bates, S.S., Hubbard, K.A., Lundholm, N., Montresor, M., Leaw, C.P., 2018. *Pseudo-nitzschia, Nitzschia*, and domoic acid: New research since 2011. Harmful Algae 79, 3–43. https://doi.org/10.1016/j.hal.2018.06.001.

Berlow, E.L., Navarrete, S.A., Briggs, C.J., Power, M.E., Menge, B.A., 1999. Quantifying variation in the strengths of species interactions. Ecology 80, 2206–2224. 10.1890/0012-9658(1999)080[2206:QVITSO]2.0.CO;2.

Bishop, I.W., Anderson, S.I., Collins, S., Rynearson, T.A., 2022. Thermal trait variation may buffer Southern Ocean phytoplankton from anthropogenic warming. Glob. Chang. Biol. 28, 5755–5767. https://doi.org/10.1111/gcb.16329.

Blanchet, F.G., Cazelles, K., Gravel, D., 2020. Co-occurrence is not evidence of ecological interactions. Ecol. Lett. 23, 1050–1063. https://doi.org/10.1111/ele.13525.

Bretherton, L., Hillhouse, J., Bacosa, H., Setta, S., Genzer, J., Kamalanathan, M., Finkel, Z.V., Quigg, A., 2019. Growth dynamics and domoic acid production of Pseudo-nitzschia sp. in response to oil and dispersant exposure. Harmful Algae 86, 55–63. https://doi.org/10.1016/j.hal.2019.05.008.

Burson, A., Stomp, M., Greenwell, E., Grosse, J., Huisman, J., 2018. Competition for nutrients and light: testing advances in resource competition with a natural phytoplankton community. Ecology. 99, 1108–1118. https://doi.org/10.1002/ecy.2187.

Cazelles, K., Araújo, M.B., Mouquet, N., Gravel, D., 2016. A theory for species co-occurrence in interaction networks. Theor. Ecol. 9, 39–48. https://doi.org/10.1007/s12080-015-0281-9.

Cembella, A., Klemm, K., John, U., Karlson, B., Arneborg, L., Clarke, D., Yamanaka, T., Cusack, C., Naustvoll, L., Bresnan, E., Šupraha, L., Lundholm, N., 2023. Emerging phylogeographic perspective on the toxigenic diatom genus *Pseudo-nitzschia* in coastal northern European waters and gateways to eastern Arctic seas: Causes, ecological consequences and socio-economic impacts. Harmful Algae 129. https://doi.org/10.1016/j.hal.2023.102496.

Delegrange, A., Lefebvre, A., Gohin, F., Courcot, L., Vincent, D., 2018. *Pseudo-nitzschia* sp. diversity and seasonality in the southern North Sea, domoic acid levels and associated phytoplankton communities. Estuar. Coast. Shelf Sci. 214, 194–206. https://doi.org/10.1016/j.ecss.2018.09.030.

Deyle, E.R., May, R.M., Munch, S.B., Sugihara, G., 2016. Tracking and forecasting ecosystem interactions in real time. Proc. R. Soc. B Biol. Sci. 283, 20152258. https://doi.org/10.1098/rspb.2015.2258.

Díaz, P.A., Álvarez, G., Figueroa, R.I., Garreaud, R., Pérez-Santos, I., Schwerter, C., Díaz, M., López, L., Pinto-Torres, M., Krock, B., 2023. From lipophilic to hydrophilic toxin producers: Phytoplankton succession driven by an atmospheric river in western Patagonia. Mar. Pollut. Bull. 193, 115214. https://doi.org/10.1016/j.marpolbul.2023.115214.

Dong, H.C., Lundholm, N., Teng, S.T., Li, A., Wang, C., Hu, Y., Li, Y., 2020. Occurrence of *Pseudo-nitzschia* species and associated domoic acid production along the Guangdong coast, South China Sea. Harmful Algae 98, 101899. https://doi.org/10.1016/j.hal.2020.101899.

Fire, S.E., Wang, Z., Byrd, M., Whitehead, H.R., Paternoster, J., Morton, S.L., 2011. Co-occurrence of multiple classes of harmful algal toxins in bottlenose dolphins (*Tursiops truncatus*) stranding during an unusual mortality event in Texas, USA. Harmful Algae 10, 330–336. https://doi.org/10.1016/j.hal.2010.12.001.

Freilich, M.A., Wieters, E., Broitman, B.R., Marquet, P.A., Navarrete, S.A., 2018. Species co-occurrence networks: Can they reveal trophic and non-trophic interactions in ecological communities? Ecology. 99, 690–699. https://doi.org/10.1002/ecy.2142.

Fritz, L., Quilliam, M.A., Wright, J.L.C., Beale, A.M., Work, T.M., 1992. An outbreak of domoic acid poisoning attributed to the pennate diatom *Pseudonitzschia australis*. J. Phycol. 28, 439–442. https://doi.org/10.1111/j.0022-3646.1992.00439.x.

Hansen, P.J., 2011. The role of photosynthesis and food uptake for the growth of marine mixotrophic dinoflagellates. J. Eukaryot. Microbiol. 58, 203–214. https://doi.org/10.1111/j.1550-7408.2011.00537.x.

Houliez, E., Schmitt, F.G., Breton, E., Skouroliakou, D.-I., Christaki, U., 2023. On the conditions promoting *Pseudo-nitzschia* spp. blooms in the eastern English Channel and southern North Sea. Harmful Algae 125, 102424. https://doi.org/10.1016/j.hal.2023.102424.

Hubbard, K.A., Villac, M.C., Chadwick, C., DeSmidt, A.A, Flewelling, L., Granholm, A., Joseph, M., Wood, T., Fachon, E., Brosnahan, M.L., Richlen, M., Pathare, M., Stockwell, D., Lin, P., Bouchard, J.N, Pickart, R., Anderson, D.M., 2023. Spatiotemporal transitions in Pseudo-nitzschia species assemblages and domoic acid along the Alaska coast. e0282794 PLoS. One 18. https://doi.org/10.1371/journal.pone.0282794.

Huisman, J., Jonker, R.R., Zonneveld, C., Weissing, F.J., 1999. Competition for Light between Phytoplankton Species: Experimental Tests of Mechanistic Theory. Ecology 80, 211–222. https://doi.org/10.2307/176991.

Huisman, J., Sharples, J., Stroom, J.M., Visser, P.M., Kardinaal, W.E.A., Verspagen, J.M. H., Sommeijer, B., 2004. Changes in turbulent mixing shift competition for light between phytoplankton species. Ecology. 85, 2960–2970. https://doi.org/10.1890/03-0763.

Ives, A.R., Dennis, B., Cottingham, K.L., Carpenter, S.R., 2003. Estimating community stability and ecological interactions from time-series data. Ecol. Monogr. 73, 301–330. https://doi.org/10.1890/0012-9615(2003)073[0301:ECSAEI]2.0.CO;2.

Kazamia, E., Helliwell, K.E., Purton, S., Smith, A.G., 2016. How mutualisms arise in phytoplankton communities: building eco-evolutionary principles for aquatic microbes. Ecol. Lett. 19, 810–822. https://doi.org/10.1111/ele.12615.

Kelly, K.J., Mansour, A., Liang, C., Kim, A.M., Mancini, L.A., Bertin, M.J., Jenkins, B.D., Hutchins, D.A., Fu, F-X., 2023. Simulated upwelling and marine heatwave events promote similar growth rates but differential domoic acid toxicity in *Pseudo-nitzschia australis*. Harmful Algae 127, 102467. https://doi.org/10.1016/j.hal.2023.102467.

Koester, I., Quinlan, Z.A., Nothias, L-F., White, M.E., Rabines, A., Petras, D., Brunson, J. K., Dührkop, K., Ludwig, M., Böcker, S., Azam, F., Allen, A.E., Dorrestein, P.C., Aluwihare, L.I., 2022. Illuminating the dark metabolome of *Pseudo-nitzschia*–microbiome associations. Environ. Microbiol. 24, 5408–5424. https://doi.org/10.1111/1462-2920.16242.

Legrand, C., Rengefors, K., Fistarol, G.O., Granéli, E., 2003. Allelopathy in phytoplankton - Biochemical, ecological and evolutionary aspects. Phycologia 42, 406–419. https://doi.org/10.2216/i0031-8884-42-4-406.1.

Likumahua, S., de Boer, M.K., Krock, B., Nieuwenhuizen, T., Tatipatta, W.M., Hehakaya, S., Imu, L., Abdul, M.S., Moniharapon, E., Buma, A.G.J., 2019. First record of the dynamics of domoic acid producing *Pseudo-nitzschia* spp. in Indonesian waters as a function of environmental variability. Harmful Algae 90, 101708. https://doi.org/10.1016/j.hal.2019.101708.

Lima, M.J., Relvas, P., Barbosa, A.B., 2022. Variability patterns and phenology of harmful phytoplankton blooms off southern Portugal: Looking for region-specific environmental drivers and predictors. Harmful Algae 116, 102254. https://doi.org/10.1016/j.hal.2022.102254.

Ljubešić, Z., Bosak, S., Viličić, D., Borojević, K.K., Marić, D., Godrijan, J., Ujević, I., Peharec, P., Đakovac, T., 2011. Ecology and taxonomy of potentially toxic *Pseudo-nitzschia* species in Lim Bay (north-eastern Adriatic Sea). Harmful. Algae 10, 713–722. https://doi.org/10.1016/j.hal.2011.06.002.

Louw, D.C., Doucette, G.J., Lundholm, N., 2018. Morphology and toxicity of *Pseudo-nitzschia* species in the northern benguela upwelling system. Harmful Algae 75, 118–128. https://doi.org/10.1016/j.hal.2018.04.008.

Lundholm, N., Krock, B., John, U., Skov, J., Cheng, J., Pančić, M., Wohlrab, S., Rigby, K., Nielsen, T.G., Selander, E., Harðardóttir, S., 2018. Induction of domoic acid production in diatoms—Types of grazers and diatoms are important. Harmful Algae 79, 64–73. https://doi.org/10.1016/j.hal.2018.06.005.

Moritz, S, Bartz-Beielstein, T., 2017. imputeTS: time series missing value imputation in R. The R Journal. 9, 207–218. https://doi.org/10.32614/RJ-2017-009.

Olesen, A.J., Ryderheim, F., Krock, B., Lundholm, N., Kiørboe, T., 2022. Costs and benefits of predator-induced defence in a toxic diatom. Proc. R. Soc. B Biol. Sci. 289, 20212735 https://doi.org/10.1098/rspb.2021.2735.

Prince, E., Irmer, F., Pohnert, G., 2013. Domoic acid Improves the competitive ability of *Pseudo-nitzschia delicatissima* against the diatom *Skeletonema marinoi*. Mar. Drugs 11, 2398–2412. https://doi.org/10.3390/md11072398.

R Core Team. 2021. R: A language and environment for statistical computing. R Foundation for Statistical Computing, Vienna, Austria. URL https://www.R-project.org/.

Roche, K.M., Sterling, A.R., Rynearson, T.A., Bertin, M.J., Jenkins, B.D., 2022. A decade of time series sampling reveals thermal variation and shifts in *Pseudo-nitzschia* species composition that contribute to harmful algal blooms in an eastern US estuary. Front. Mar. Sci. 9, 1–11. https://doi.org/10.3389/fmars.2022.889840.

Rue, E., Bruland, K., 2001. Domoic acid binds iron and copper: A possible role for the toxin produced by the marine diatom *Pseudo-nitzschia*. Mar. Chem. 76, 127–134. https://doi.org/10.1016/S0304-4203(01)00053-6.

Rynearson, T.A., Flickinger, S.A., Fontaine, D.N., 2020. Metabarcoding reveals temporal patterns of community composition and realized thermal niches of *Thalassiosira* spp. (Bacillariophyceae) from the Narragansett Bay long-term plankton time series. Biology 9, 19. https://doi.org/10.3390/biology9010019.

Sampaio, E., Gallo, F., Schulz, K.G., Azevedo, E.B., Barcelos, J., 2017. Phytoplankton interactions can alter species response to present and future CO2 concentrations. Mar. Ecol. Prog. Ser. 575, 31–42. https://doi.org/10.3354/meps12197.

Sandoval-Belmar, M., Smith, J., Moreno, A.R., Anderson, C., Kudela, R.M., Sutula, M., Kessouri, F., Caron, D.A., Chavez, F.P., Bianchin.D., 2023. A cross-regional examination of patterns and environmental drivers of *Pseudo-nitzschia* harmful algal blooms along the California coast. Harmful Algae 126, 102435. 10.1016/j.hal.2023.102435.

Sauvey, A., Claquin, P., Roy, B.Le, Jolly, O., Fauchot, J., 2023. Physiological conditions favorable to domoic acid production by three *Pseudo-nitzschia* species. J. Exp. Mar. Bio. Ecol. 559, 151851 https://doi.org/10.1016/j.jembe.2022.151851.

Seeyave, S., Probyn, T.A., Pitcher, G.C., Lucas, M.I., Purdie, D.A., 2009. Nitrogen nutrition in assemblages dominated by *Pseudo-nitzschia* spp., *Alexandrium catenella* and *Dinophysis acuminata* off the west coast of South Africa. Mar. Ecol. Prog. Ser. 379, 91–107. https://doi.org/10.3354/meps07898.

Smith, A.N., Hennon, G.M.M., Zinser, E.R., Calfee, B.C., Chandler, J.W., Barton, A.D., 2021. Comparing *Prochlorococcus* temperature niches in the lab and across ocean basins. Limnol. Oceanogr. 66, 2632–2647. https://doi.org/10.1002/lno.11777.

Sonnet, V., Guidi, L., Mouw, C.B., Puggioni, G., Ayata, S.D., 2022. Length, width, shape regularity, and chain structure: time series analysis of phytoplankton morphology from imagery. Limnol. Oceanogr. 67, 1850–1864. https://doi.org/10.1002/lno.12171.

Sosik, H.M., Olson, R.J., 2007. Automated taxonomic classification of phytoplankton sampled with imaging-in-flow cytometry. Limnol. Oceanogr. Methods 5, 204–216. https://doi.org/10.4319/lom.2007.5.204.

Sterling, A.R., Kirk, R.D., Bertin, M.J., Rynearson, T.A., Borkman, D.G., Caponi, M.C., Carney, J., Hubbard, K.A., King, M.A., Maranda, L., McDermith, E.J., Santos, N.R., Strock, J.P., Tully, E.M., Vaverka, S.B., Wilson, P.D., Jenkins, B.D., 2022. Emerging harmful algal blooms caused by distinct seasonal assemblages of a toxic diatom. Limnol. Oceanogr. 67, 2341–2359. https://doi.org/10.1002/lno.12189.

Stoecker, D.K., Hansen, P.J., Caron, D.A., Mitra, A., 2017. Mixotrophy in the Marine Plankton. Ann. Rev. Mar. Sci. 9, 311–335. https://doi.org/10.1146/annurev-marine-010816-060617.

Stonik, I.V., Orlova, T.Y., Shevchenko, O.G., 2001. Morphology and Ecology of the Species of the Genus *Pseudo-nitzschia* (Bacillariophyta) from Peter the Great Bay, Sea of Japan. Russ. J. Mar. Biol. 27, 362–366. https://doi.org/10.1023/A:1013701403968.

Trimborn, S., Brenneis, T., Sweet, E., Rost, B., 2013. Sensitivity of Antarctic phytoplankton species to ocean acidification: Growth, carbon acquisition, and species interaction. Limnol. Oceanogr. 58, 997–1007. https://doi.org/10.4319/lo.2013.58.3.0997.

Velo-Suárez, L., González-Gil, S., Gentien, P., Lunven, M., Bechemin, C., Fernand, L., Raine, R., Reguera, B., 2008. Thin layers of *Pseudo-nitzschia spp.* and the fate of *Dinophysis acuminata* during an upwelling-downwelling cycle in a Galician Ría. Limnol. Oceanogr. 53, 1816–1834. https://doi.org/10.4319/lo.2008.53.5.1816.

Wells, M.L., Trick, C.G., Cochlan, W.P., Hughes, M.P., Trainer, V.L., 2005. Domoic acid: The synergy of iron, copper, and the toxicity of diatoms. Limnol. Oceanogr. 50, 1908–1917. https://doi.org/10.4319/lo.2005.50.6.1908.

Wickham, H., 2016. ggplot2: Elegant Graphics for Data Analysis. Springer-Verlag, New York. https://ggplot2.tidyverse.org.

Wilke, Claus O.. cowplot: Streamlined Plot Theme and Plot Annotations for 'ggplot2'. R package version 1.1.1. https://wilkelab.org/cowplot/.

Wohlrab, S., John, U., Klemm, K., Eberlein, T., Grivogiannis, A.M.F., Krock, B., Frickenhaus, S., Bach, L.T., Rost, B., Riebesell, U., Van de Waal, D.B., 2020. Ocean acidification increases domoic acid contents during a spring to summer succession of coastal phytoplankton. Harmful. Algae 92, 101697. https://doi.org/10.1016/j.hal.2019.101697.

Xu, D., Zheng, G., Brennan, G., 2023. Plastic responses lead to increased neurotoxin production in the diatom *Pseudo-nitzschia* under ocean warming and acidification. ISME J. 17, 525–536. https://doi.org/10.1038/s41396-023-01370-8.

Xu, N., Tang, Y.Z., Qin, J., Duan, S., Gobler, C.J., 2015. Ability of the marine diatoms *Pseudo-nitzschia multiseries* and *P. pungens* to inhibit the growth of co-occurring phytoplankton via allelopathy. Aquat. Microb. Ecol. 74, 29–41. https://doi.org/10.3354/ame01724.